An Alternative Strategy to Control the Electronic Properties of Bilayer Graphene: Semi-metal to Metal Transition and a Rare 2D Material with Dirac Cone

Srimanta Pakhira,[1,2] Kevin P. Lucht,[1,2] and Jose L. Mendoza-Cortes[1,2,*]

[1] *Condensed Matter Theory, National High Magnetic Field Laboratory, Scientific Computing Department, Materials Science and Engineering, Florida State University, Tallahassee FL, 32310, USA*

[2] *Department of Chemical & Biomedical Engineering, FAMU-FSU Joint College of Engineering, Florida State University, Tallahassee FL, 32310, USA.*

(Dated: October 18, 2016)

The AB-stacked bilayer graphene (BLG) is a pure semiconductor whose band gap and properties can be tuned by various methods such as doping or applying gate voltage. Here we show an alternative method to control the electronic properties of bilayer graphene by adding transition metal atoms between the two graphene monolayers. A theoretical investigation of two-dimensional (2D) monolayer graphene (MLG), BLG, BLG with one Vanadium (V) atom (BLG-1V), BLG with two V atoms (BLG-2V) and BLG with three V atoms (BLG-3V) nanostructured materials, all of which are energetically stable, have been performed using dispersion-corrected DFT method. Our study reveals that the only MLG and BLG-1V materials have a Dirac Cone at the K-point. We have demonstrated that the material properties such as Dirac Cone of the BLG-intercalated materials can be tuned by adding V atoms between two graphene layers in one unit cell. Thus we show a new strategy to control the electronic properties of bilayer graphene, and by varying the concentration of Vanadium atom in unit cell, the electronic properties can be modulated between metallic, semi-metallic and semi-conducting. In all the cases, the present DFT calculations show that the $2p_z$ sub-shell of 2p orbital of the C atoms in graphene and the $3d_{yz}$ sub-shell of 3d orbital provide the electron density near to Fermi level resulting aforementioned material properties of the BLG-intercalated materials.

arXiv:1610.04777v1 [cond-mat.mtrl-sci] 15 Oct 2016

In modern science and technology, there has been a tremendous and huge amount of theoretical and experimental interest in the low energy electronic properties of ultrathin graphite films including graphene monolayer and graphene bilayer materials. Graphene [1], a two-dimensional (2D) honeycomb sheet of carbon just one atom thick with hybridized sp^2 bonded orbitals between carbon atoms [2], is an ideal and novel material for making nanoelectronic and photonic devices in modern science and technology, because it is a very good electrical conductor as well as being the thinnest 2D material known. Graphene has a unique linear band structure around the Fermi level (E_F) forming a Dirac Cone at the K-points of its Brillouin zone, and has led to fascinating phenomena, exemplified by massless Dirac fermion physics [3–6]. The Dirac Cone which represents linear energy dispersion at Fermi level gives graphene massless fermions, leading to various quantum Hall effects, ultra high carrier mobility, and many other novel phenomena and properties. The Dirac Cones are highly sensitive and rare, it is highly dependent on the symmetry, parameters, Fermi energy level, and band structures of the materials. The presence of Dirac Cone in graphene [4] has attracted a lot of research interest in modern science and technology because of its intriguing physics as well its potential applications in many areas of science, nano-technology and industry [7].

Single layer or monolayer graphene (SLG or MLG) has an electronic structure that can be controlled by an electrical field [8]. The strength and conductive efficiency of the one atom thick carbon-based material makes it an attractive contender for new faster and more efficient microchips and nanochips. To be used in digital electronics, however, MLG has the well known zero-gap issue [9] which makes the achievement of a high on-off ratio difficult deeming it unsuitable for transistors, which are the foundation of all modern electronic devices. To solve this problem, bilayer graphene (BLG) can be used instead of MLG, with a gap opening simply by applying an electric field [10, 11]. With one more graphene layer added, bilayer graphene has an entirely different band structure and equally interesting [12], since the band gap of the BLG can be modulated from zero to a few eV by using different methods such as doping, applying an external electric field etc. In addition, BLG holds potential for electronics and nano-technological applications, particularly because of the possibility to control both carrier density and energy band gap through doping or gating [3, 4, 13, 14]. The most remarkable thing is that the inversion symmetric AB-stacked bilayer graphene is a zero-band gap semiconductor in its pristine form. But a non-zero band gap can be induced by breaking the inversion symmetry of the two graphene monolayers to form AA-stacked BLG. When two graphene monolayers are stacked (in both the cases AA- and AB-stacked BLG), the monolayer features are lost and dispersion effects become quadratic and more effective [13]. Thus, BLG acts as semiconductor and exhibits an electric field-induced,

* Corresponding Author: Prof. J. L. Mendoza-Cortes, email: jmendozacortes@fsu.edu

broadly tunable band gap [4]. Because tuning the band gap of bilayer graphene can turn it from a semiconductor into a metal or semi-metal, a single millimeter-square sheet of bilayer graphene could potentially hold millions of differently tuned electronic devices that can be reconfigured. Recently, laseres have been used to get BLG to act as a conductor, Dirac material or semiconductor, an important step towards computer chips made of an excellent 2D material [15].

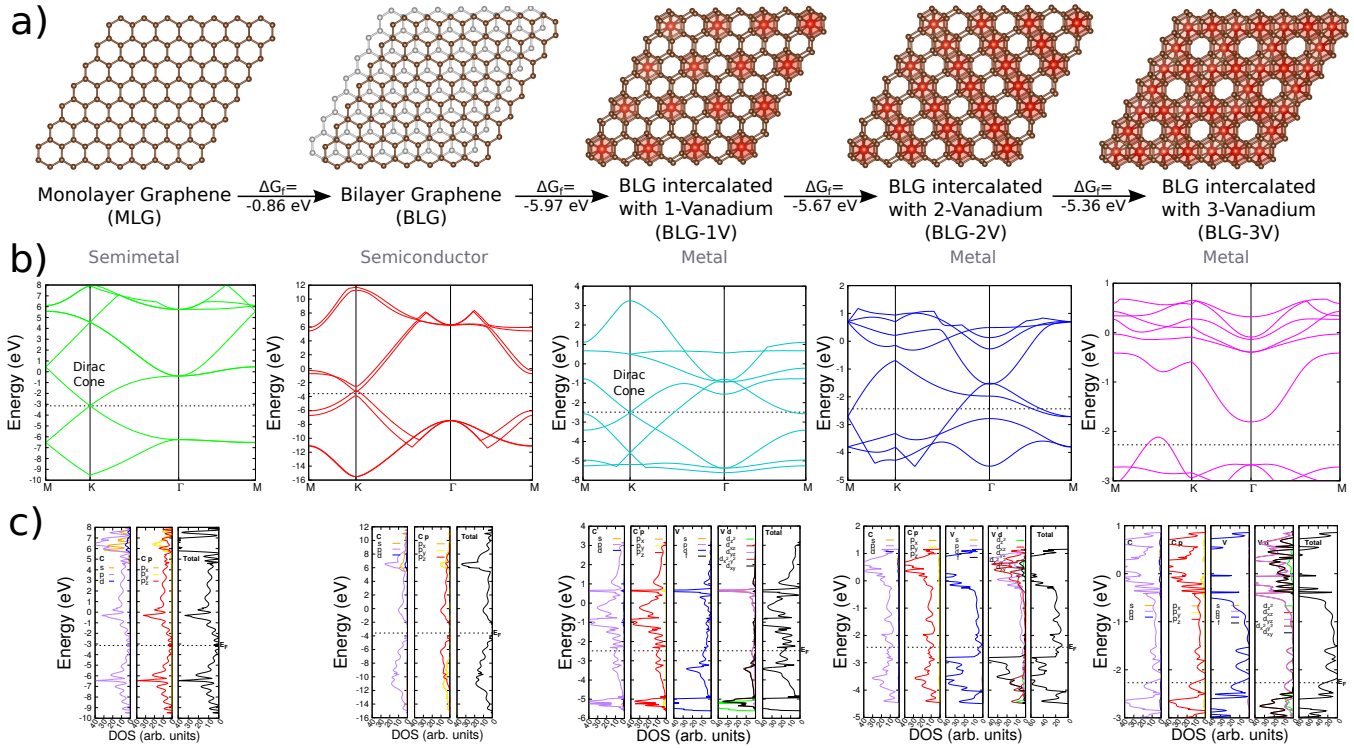

FIG. 1. (a) The optimized structures of MLG, BLG, BLG-1V, BLG-2V, and BLG-3V 2D materials. (First row in Top). (b) The band structures of these materials. (Second row). (c) The density of states (DOSs) of these materials are at the bottom (third row). The individual components of DOSs of the C and V atoms, and total DOSs (depicted by "Total" in the third row) are also presented in here. All the compounds shown above are stable by the means of the calculation of their vibrational mode, i.e. no imaginary frequency was found. The addition of a 4th Vanadium atom was calculated and it was found to be an unstable structure.

In this Letter we show, theoretically, that the band structure of BLG can be controlled by adding Vanadium (V) metal atom between two graphene layers so that the electronic band gap between the valence and conduction bands can be tuned and a Dirac Cone appears. This makes BLG/BLG-intercalated a promising material with a tunable energy gap and may open a new door for developing new modern electronic devices. We also show that the band gap depends on the coupling between the two graphene layers and symmetry of the BLG system i.e. AB stacking and AA stacking. By the definition of the intercalation of a nanostructured material, one layer of metal atoms is intercalated between two graphene monolayers (it consists of two or more graphene monolayers embedded by a layer of metal atoms between the graphene monolayers). Intercalation of Vanadium atoms between a graphene bilayer causes surprisingly very high electronic conductivity. We have performed a theoretical investigation of electronic structures, material properties such as band structure, projected density of states (DOSs), band gap and structural stability of the monolayer graphene, bilayer graphene, BLG intercalated with one Vanadium atom (BLG-1V), BLG intercalated with two Vanadium atoms (BLG-2V), and BLG intercalated with three Vanadium atoms (BLG-3V) using dispersion-corrected hybrid DFT method [16–21]. Various types of BLG with Vanadium materials have been computationally prepared by the atomic intercalation of Vanadium atoms between the graphene monolayers, which consequently result in various nanostructured periodic 2D materials. We have also investigated their structural stabilities by computing the relative Gibbs free energies or formation energy (ΔG_f) and binding energies (ΔE) of the aforementioned systems.

The geometrical and crystal structure of the MLG, BLG and BLG-intercalated materials (BLG-1V, BLG-2V and BLG-3V) were optimized by the dispersion-corrected B3LYP hybrid density functional theory (DFT) [16–18], i.e. B3LYP-D2 [19–21] which has been shown to give correct electronic properties of 2D materials [22]. The semi-

TABLE I. Bond distances and lattice constants of the MLG, BLG, BLG-1V, BLG-2V, and BLG-3V 2D materials. The d is defined as the interlayer distance between the monolayers.

Component	C-C (Å)	C-V (Å)	a (Å)	b (Å)	d(Å)
MLG	1.416	N/A	2.451	2.451	N/A
BLG	1.421	N/A	2.449	2.449	3.390
BLG-1V	1.439	2.243	8.561	4.942	3.441
BLG-2V	1.442	2.335	8.575	5.022	3.645
BLG-3V	1.464	2.413	8.717	5.031	3.658

TABLE II. Relevant properties of the MLG, BLG, BLG-1V, BLG-2V, and BLG-3V 2D materials.

Component	State	ΔE (eV)	ΔG_f (eV)	Dirac Cone
MLG	Semimetal	N/A	N/A	Exist
BLG	Semiconductor	-0.93	-2.51	No
BLG-1V	Metal	-6.21	-5.97	Exist
BLG-2V	Metal	-5.95	-5.67	No
BLG-3V	Metal	-5.66	-5.36	No

empirical Grimme-D2 dispersion corrections were added in the present calculations in order to incorporate van der Waals dispersion effects on the system and to estimate the van der Waals forces [19–21]. The graphene intercalated nanostructured 2D materials (BLG-1V, BLG-2V, and BLG-3V) have been prepared by adding the V atoms in one unit cell in their crystal structures. In the present computation, triple-zeta valence with polarization quality (TZVP) Gaussian basis sets were used for both C and V atoms [24]. To optimize all the aforementioned materials, the CRYSTAL14 [23] suite code was used. In this work, AB-stacked BLG systems, and AA-stacked BLG-intercalated materials have been considered with tunable interlayer separation. The unit cell constructed this way contains one configuration, known as AA, where one atom is exactly above another atom of the other layer of graphene, there is another configuration, AB, where an atom of the top of graphene layer is exactly in the center of a lower layer hexagon as shown in Figure 1a (top left). Due to AA-stacking, the C atoms of top layer are situated just above the corresponding C atoms of the bottom layer. To reproduce previous experimental and theoretical results, we have considered both AA and AB-stacking for the BLG material, while we have used the AA-stacked layer structures for the BLG-1V, BLG-2V, and BLG-3V materials, which are the stable configurations.

The optimized geometries of the MLG, BLG, and BLG-intercalated materials along with their band structures and projected density of states (DOSs) are shown in Figure 1. The contribution of the sub-shells (such as p_x, p_y, p_z d_{yz} etc.) in the total DOSs has been also computed. The present DFT calculation shows that the Dirac Cone exist at the K-point (also known as Dirac point) in the band structure (as shown in Figure 1b) of the pristine MLG material which is consistent with the previous results [3–6]. It is found that the low-energy bands of MLG arise from the $2p_z$ sub-shells of 2p orbitals of C atoms, as depicted in the DOSs structure calculation in Figure 1c, which plays an important role to create the Dirac Cone in the band structure of the pristine MLG. The "Total" DOSs calculations show the electron density around the Fermi energy level, which make MLG as a semimetal. The C-C bond distance in MLG is about 1.416 Å, and the lattice constants (a=b) is 2.451 Å as shown in Table I, which agrees well with previous experimental results. In the pristine BLG (AB-stacked), the Fermi level lies at the point where the two low-energy bands touch (shown as zero band gap energy in Figure 1b) each other just above the E_F and, thus, this region is relevant for the study of electronic properties of it. The shape of the band structure of the BLG predicted by the present B3LYP computations is in good agreement with that calculated by previous DFT methods and experiments [25, 26]. We have also studied the AA-stacked BLG, but our computation shows that AB-stacked BLG is more stable than the AA-stacked BLG. Two bands (the valence and conduction bands) are crossing near to E_F at K-points, but both the AA- and AB-stacked BLG systems have Dirac Cone, which agree well with the previous experimental results [25, 26]. Thus the BLG is a zero-gap semiconductor. The intercalation distance, d, between the two monolayers in the AB-stacked BLG material is about 3.390 Å (as depicted in Table I) which agrees with the previous experimental and theoretical results [25]. The C-C bond distance and lattice constant (a=b) in the AB-stacked BLG are about 1.421 Å and 2.449 Å respectively (as shown in Table I). We have also calculated the formation energy (ΔG_f) of all the system studied in here. The required energy, ΔG_f, to form the AB-stacked BLG from MLG, is about -0.86 eV. The corresponding binding energy (BE) of putting together two MLG, ΔE, of BLG is about -0.93 eV as shown in Table II.

For optimal bonding between the Vanadium and graphene, the bilayer graphene follows a AA-stacking arrangement with the Vanadium placed at the center of the honeycomb. With this conformation, the Vanadium d-orbitals will be situated to favorably interact with the p_z orbital orthogonal to the graphene layer. Relative to bilayer graphene, the BLG-1V structure with a single Vanadium atom in the unit cell is highly favorable by -5.97 eV. To form the BLG-1V from the MLG with V atom and one MLG, the required ΔG_f (formation energy) and ΔE (binding energy) are -2.51 eV and -2.79 eV respectively. Additional Vanadium atoms are also favorable by -5.67 eV between single metal (to form BLG-2V material) and double metal addition, and -5.36 eV between the double metal and triple metal addition (to form BLG-3V material). And the corresponding ΔE of the BLG-1V, BLG-2V, and BLG-3V are -6.21 eV, -5.95 eV, and -5.66 eV respectively, as depicted in Table II. The formation energies, ΔG_f, of these materials are depicted in Table II and Fig 1. The intercalation distances between two graphene layers of these BLG-1V, BLG-2V and BLG-3V materials are 3.441 Å, 3.645 Å and 3.658 Å respectively, as shown in the Table I. The present DFT

calculation shows that the intercalation distances have been gradually increased in the intercalated BLG materials, BLG-1V to BLG-3V, but not equally. The bond distances (C-C and C-V) and lattice constants (a and b) of all the materials studied here are presented in Table I. Our computation shows the C-C bond distance in all the systems, BLG-1V, BLG-2V and BLG-3V, has been changed by an amount 0.043 Å due to presence of V atoms between the graphene layers. We have also prepared a structure of BLG material with four V atoms (BLG-4V), but the frequency calculations prove that the structure is highly unstable thermodynamically as it has many imaginary frequencies, and hence the result is excluded in this Letter.

The addition of Vanadium atom was found to substantially alter the electron properties in the graphene bilayer. With the addition of a single Vanadium atom in BLG (i.e. BLG-1V) material, the electron properties yields Dirac Cone along the K direction (as shown in Figure 1b) and substantial band overlap resulting in metallic behavior. The individual components of the p-orbitals electron density of C atoms in graphene and the d-orbitals electron density of V atoms have been explicitly shown along with the "Total" electron density in the DOSs computations in Figure 1c. The band structure calculations show that the two bands (valence band and conduction band) meet at K-points and at the Fermi energy level of the BLG-1V materials and formed a Dirac Cone at K-points, and therefore the K-points are also called Dirac points. This makes the BLG-1V material an excellent conductor or Dirac material with zero band gap. The present computation shows that the Dirac Cone appears in AA-stacked BLG-1V 2D material, which was disappeared in pristine AA- or AB-stacked BLG material. This calculation shows that the it is possible to form a Dirac material using bilayer graphene and one V atom per unit cell. Thus the total density of states calculations (as shown in Figure 1c labeled by "Total") show the electron distribution (or density) at and near to the Fermi level E_F. The electrons can freely move from valence band to conduction band, and it reveals that the ultrahigh intrinsic electron mobility of BLG and BLG-1V materials. So, the BLG-1V material can be used in various modern electronic devices as a 2D Dirac material. In the AA-/AB-stacked BLG material, two bands just touch each other at K-points near to the E_F, not exactly at the E_F as described earlier. Thus the BLG does not show the Dirac Cone, it is just a non-zero/zero band gap semiconductor. The DOSs structure of BLG shows that the electron in the p_z sub-shells of 2p orbitals (highlighted by red color) of the C atoms in graphene plays an important role of contributing the electron density resulting in semiconducting behavior along the K directions. Where as the DOSs calculations of the BLG-1V material show the electron density around the E_F level, and the electron density is coming from the p_z (highlighted by red color) sub-shells of p orbital electrons of C atoms in graphene and the d_{yz} (highlighted by violet color) and d_{xy} (highlighted by black color) sub-shells of d orbital electrons of V atom. The Dirac point locate at the K line, and out-of-plane of density of states (p_z orbitals from the carbon hexagons, and d_{yz} and d_{xy} sub-shells of d orbital electrons of vanadium) is solely responsible for the emergence of Dirac Cone of the BLG-1V material. This calculation proves that the BLG-1V has an excellent metallic behavior with Dirac Cone due to presence of electron density around Fermi level. Like MLG material, the BLG-1V shows low-energy fermionic excitations and it behaves as massless Dirac particles rather than fermions obeying the usual Schrdinger Hamiltonian. This emergent behavior of Dirac fermions in condensed matter systems defines the unifying framework for a class of materials we call Dirac materials.

With the addition of another Vanadium atom in BLG-1V material, the Dirac Cone disappears, and the bands shift causing the Fermi energy to be above the bottom of the conducting bands, and it forms BLG-2V materials. The band structures and DOSs show the cause of metallic behavior of the BLG-2V materials. The metallic behavior of the BLG-2V material has been found along the Γ as well as K directions as shown in band structure of it. The band structure of the BLG-2V materials also shows the two valence bands are crossing the Fermi level resulting an electron density around E_F. The "Total" density of states show the electron distribution at the Fermi level. The DOSs structure calculations shows that the electron density is coming mainly from the p_z subshell of 2p orbital electrons of C atoms in graphene and the d_{yz} orbital electrons of V atom. So, BLG-2V shows the metallic behavior. And lastly, with three Vanadium atoms in one unit cell, a small indirect band gap appears with the Fermi energy slightly below the top of the valence band. But the one valence band is crossing the Fermi level along the M to K directions, it makes an electron distribution near to E_F as shown in DOSs calculations, thus resulting this BLG-3V material as a metal or semi-metal. The DOSs calculations show that electron distribution or density around the Fermi level due to the p_z sub-shell of 2p orbital electrons of C atoms in graphene and the d_{yz} sub-shell of 3d orbital electrons of V atoms. So, among all the intercalated materials, BLG-3V shows less electron density near to E_F.

An alternative method of controlling the electron properties of GVG materials is by altering the spin conformation. All previous materials have referenced Vanadium in the high-spin state, and in the case of BLG-2V and BLG-3V in a ferromagnetic (FM) spin arrangement. Considering an anti-ferromagnetic (AFM) arrangement of spins, we can drastically modify the properties. Figure 3 shows the band structure and DOSs of the AFM BLG-2V material. In the case of BLG-2V, the AFM conformation yields greater spin densities of 2.22 μ_B and -2.22 μ_B compared to the FM conformation with 1.86 μ_B for each Vanadium. Relative to its FM counterpart, the AFM BLG-2V structure is more stable by ΔG_f = -0.410 eV. Examining the electronic properties, we no-

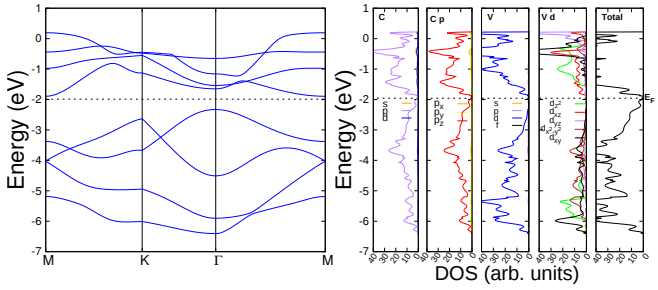

FIG. 2. The band structure and density of state (DOSs) of the alpha electron of AFM (anti-ferromagnetic) BLG-2V materials are presented. The beta electrons exhibit identical information. The individual components of DOSs of the C and V atoms, and total DOSs (depicted by "Total" in the third row) are also presented here. Compared to FM (ferromagnetic) BLG-2V, the Dirac Cone disappears and a band gap appears.

tice considerable differences between the AFM and FM BLG-2V structures. Once in the AFM state, BLG-2V not only loses its Dirac Cone, but also creates a degenerate pair of band structures (for alpha and beta electrons) with a band opening between the valence and conductive band. The band gaps of this spacing are 0.101 eV for the indirect transition and 0.681 eV for the direct transition. This study shows that not only are the electronic properties of BLG-intercalated systems dependent on the concentration of Vanadiums intercalated between BLG, but also on the arrangement on the spins, which adds an additional variable to modifying the behavior of BLG-intercalated systems.

In summary, we have theoretically studied the MLG, BLG, BLG-intercalated nanostructured 2D materials using dispersion corrected B3LYP method with TZVP basis sets. The band and DOSs structures have been calculated in the present calculations. The individual components of the sub-shells of the p-orbitals (i.e. p_x, p_y and p_z) of C atoms and the d-orbitals (i.e. d_{z^2}, d_{xz}, d_{yz}, $d_{x^2-y^2}$, and d_{xy}) of the V atoms, which are taking part in the total electron density in DOSs have also reported along with the DOSs calculations. Among all the systems, MLG and BLG-1V materials have Dirac Cone at the K-point, and more interestingly we have found that the BLG-3V material shows the electron density has been decreased near to Fermi energy level, and the Dirac Cone disappears. To conclude, this work provides the first theoretical investigation on the BLG with the intercalated one, two and three V atoms per unit cell and the first observation of Dirac Cone in the BLG-1V nanostructured material. It further shows that the how the material properties have been changed in BLG, MLG, BLG-1V, BLG-2V and BLG-3V systems due to presence of Vanadium atoms and Dirac Cone move. More interestingly, we observe that the V 3d shells receive more electron donation from the graphene $2p_z$ sub-shell of 2p orbital, which causes greater different between electron distributions of spin-up and spin-down in the partially filled 3d orbitals in V atom. We have also found that the $2p_z$ sub-shell of orbital of C atom and $3d_{yz}$ sub-shell of 3d orbital of the V atoms in the MLG, BLG, BLG-1V, BLG-2V, and BLG-3V materials play the main important role to show the Dirac Cone and the conducting properties. We show an alternative method of controlling the electronics and material properties of BLG-intercalated materials is by altering the spin conformation. It reveals that the AFM arrangement of spins of the BLG-2V material has changed it to semi-conductor with small band gap from metal. In conclusion, Dirac Cone structure gives the MLG and BLG-1V materials massless fermions leading to ultrahigh carrier mobility. The present study reveals that the material properties of the BLG material can be controlled by adding the V atoms per unit cell for the first time. We can also conclude that BLG-1V, a Dirac material offers us a guidance in predicting the new features that we have established to be universal, just like the currently well known Dirac materials which play an important role in modern material science. This study may allow bilayer graphene, the only known semiconductor with a tunable energy gap, new avenues to develop 2D Dirac materials and modern electronic devices.

[1] K. S. Novoselov, J. M. Raimond, M. Brune, Q. Computation, F. D. Martini, C. Monroe, D. L. Moehring, P. L. Knight, M. B. Plenio, V. Vedral, E. S. Polzik, C. Variables, S. L. Braunstein, A. K. Pati, M. D. Lukin, I. J. Cirac, P. Zoller, C. Han, P. Xue, G. C. Guo, S. V. Polyakov, A. Kuzmich, H. J. Kimble, J. I. Cirac, T. A. B. Kennedy, P. Horodecki, R. Horodecki, D. P. Divincenzo, J. A. Smolin, A. Beige, L. C. Kwek, P. Kok, J. A. Sauer, L. You, A. Zangwill, M. S. Chapman, M. Nielsen, A. K. Geim, S. V. Morozov, D. Jiang, Y. Zhang, S. V. Dubonos, I. V. Grigorieva, and A. A. Firsov, Science **306**, 666 (2004).

[2] A. H. Castro Neto, F. Guinea, N. M. R. Peres, K. S. Novoselov, and A. K. Geim, Reviews of Modern Physics **81**, 109 (2009), arXiv:0709.1163.

[3] T. Ohta, Science **313**, 951 (2006), arXiv:arXiv:1011.1669v3.

[4] E. V. Castro, K. S. Novoselov, S. V. Morozov, N. M. R. Peres, J. M. B. L. Dos Santos, J. Nilsson, F. Guinea, A. K. Geim, and A. H. C. Neto, Physical Review Letters **99**, 8 (2007), arXiv:0611342 [cond-mat].

[5] S. Y. Zhou, G.-H. Gweon, a. V. Fedorov, P. N. First, W. a. de Heer, D.-H. Lee, F. Guinea, a. H. Castro Neto, and a. Lanzara, Nature materials **6**, 770 (2007), arXiv:0709.1706.

[6] K. Mullen, B. Uchoa, and D. T. Glatzhofer, Physical Review Letters **115**, 1 (2015), arXiv:1408.5522.

[7] K. S. Novoselov, A. K. Geim, S. V. Morozov, D. Jiang,

M. I. Katsnelson, I. V. Grigorieva, S. V. Dubonos, and A. A. Firsov, Nature **438**, 197 (2005), arXiv:0509330 [cond-mat].
[8] K. S. Novoselov, V. I. Fal'ko, L. Colombo, P. R. Gellert, M. G. Schwab, and K. Kim, Nature **490**, 192 (2012).
[9] P. Avouris, Nano Letters **10**, 4285 (2010).
[10] J. B. Oostinga, H. B. Heersche, X. Liu, A. F. Morpurgo, and L. M. K. Vandersypen, Nature materials **7**, 151 (2008), arXiv:0707.2487.
[11] E. McCann, Physica Status Solidi (B) Basic Research **244**, 4112 (2007), arXiv:0608221 [cond-mat].
[12] T. Ohta, A. Bostwick, J. L. McChesney, T. Seyller, K. Horn, and E. Rotenberg, Physical Review Letters **98**, 16 (2007), arXiv:0612173 [cond-mat].
[13] E. McCann and V. I. Fal'ko, Physical Review Letters **96**, 1 (2006), arXiv:0510237 [cond-mat].
[14] K. S. Novoselov, E. McCann, S. V. Morozov, V. I. Falko, M. I. Katsnelson, U. Zeitler, D. Jiang, F. Schedin, and a. K. Geim, Nat. Phys. **180**, 177 (2006), arXiv:0602565 [cond-mat].
[15] Z. Lin, X. Ye, J. Han, Q. Chen, P. Fan, H. Zhang, D. Xie, H. Zhu, and M. Zhong, Scientific reports **5**, 11662 (2015).
[16] A. D. Becke, The Journal of Chemical Physics **98**, 5648 (1993), arXiv:z0024.
[17] A. D. Becke, Physical Review A **38**, 3098 (1988), arXiv:PhysRevA.38.3098 [10.1103].
[18] C. Lee, W. Yang, and R. G. Parr, Physical Review B **37**, 785 (1988), arXiv:PhysRevA.38.3098 [10.1103].
[19] S. Grimme, Journal of Computational Chemistry (2006), 10.1002/jcc.20495, arXiv:NIHMS150003.
[20] S. Pakhira, C. Sahu, K. Sen, and A. K. Das, Chemical Physics Letters **549**, 6 (2012).
[21] S. Pakhira, K. Sen, C. Sahu, and A. K. Das, The Journal of chemical physics **138**, 164319 (2013).
[22] K. P. Lucht and J. L. Mendoza-Cortes, Journal of Physical Chemistry C **119**, 22838 (2015).
[23] R. Dovesi, R. Orlando, B. Civalleri, V. R. Saunders, and C. M. Zicovich-Wilson, **220**, 571 (2005).
[24] M. F. Peintinger, D. V. Oliveira, and T. Bredow, Journal of Computational Chemistry **34**, 451 (2013).
[25] H. Min, B. Sahu, S. K. Banerjee, and A. H. MacDonald, Physical Review B - Condensed Matter and Materials Physics **75**, 1 (2007), arXiv:0612236 [cond-mat].
[26] S. Latil and L. Henrard, Physical Review Letters **97**, 1 (2006).